

**IMPACT OF PRESSURIZED EXTRACTION AND
ELECTROHYDRODYNAMIC ENCAPSULATION
METHODS ON ANTIOXIDATIVE PROPERTIES
OF *MOMORDICA CHARANTIA* FRUIT EXTRACT**

AMIREHSAN TORKAMANI

UNIVERSITI SAINS MALAYSIA

2018

**IMPACT OF PRESSURIZED EXTRACTION AND
ELECTROHYDRODYNAMIC ENCAPSULATION
METHODS ON ANTIOXIDATIVE PROPERTIES
OF *Momordica charantia* L. FRUIT EXTRACT**

by

AMIREHSAN TORKAMANI

Thesis submitted in fulfillment of the requirements

for the degree of

Doctor of Philosophy

April 2018

ACKNOWLEDGEMENT

First and foremost, I offer my sincerest gratitude to my mother, father and sister who have supported me throughout this stage of my life unsparingly and I attribute my thesis to them.

Furthermore, I am deeply grateful and indebted to my supervisors Prof. Dr. Norziah binti Mohd Hani, Dr. Syahariza binti Zainul Abidin, Prof. Dr. Wan Ahmad Kamil bin Che Mahmood and Dr. Pablo Juliano for their help and support throughout this wonderful and often overwhelming experience.

I would like to extend my gratitude to Universiti Sains Malaysia (USM) for providing the financial support under Research University Individual Fund (RUI) and USM Postgraduate Fellowship scholarship. In addition, my appreciations go to the staff at Food Technology Division and School of Chemical Sciences, USM who have made my stay enjoyable and memorable.

TABLE OF CONTENTS

ACKNOWLEDGEMENT	ii
TABLE OF CONTENTS	iii
LIST OF TABLES	x
LIST OF FIGURES	xi
LIST OF ABBREVIATIONS	xvi
ABSTRAK	xx
ABSTRACT	xxii
CHAPTER 1 - INTRODUCTION	
1.1 Background	1
1.2 Objectives	3
CHAPTER 2 - LITERATURE REVIEW	
2.1 Bitter Gourd.....	4
2.1.1 Etymology and Morphology	4
2.1.2 Medicinal applications of BG	5
2.2 BG antioxidant profile	7
2.3 Downstream processes of bioactive compounds	8
2.3.1 BG bioactive compound extraction methods	8
2.3.2 Ultrasound Assisted Extraction (UAE).....	10
2.3.3 Pressurized Liquid Extraction (PLE)	19

2.4	Encapsulation processes	23
2.4.1	Electrohydrodynamic Technologies.....	24
2.4.2	Parameters affecting electrohydrodynamic processes	26
2.4.3	Encapsulation application of electrohydrodynamic techniques in food sector	29

CHAPTER 3 - CHARACTERIZATION AND OPTIMIZATION OF ULTRASONIC ASSISTED EXTRACTION OF ANTIOXIDATIVE POLYPHENOLIC COMPOUNDS OBTAINED FROM MOMORDICA CHARANTIA

3.1	Introduction	32
3.2	Materials and methods.....	32
3.2.1	Chemicals and reagents.....	32
3.2.2	Plant material	33
3.2.3	Ultrasound system and extraction reactor setup.....	33
3.2.4	Ultrasound field characterization	34
3.2.5	Extraction method	34
3.2.6	Total phenolic content (TPC).....	35
3.2.7	Total flavonoid content (TFC)	36
3.2.8	Ferric reducing/antioxidant power assay (FRAP assay)	37
3.2.9	Free radical scavenging activity by DPPH method.....	37
3.2.10	Experimental design and statistical analysis	38

3.3	Results and Discussion	40
3.3.1	Single factor analysis (SFA)	40
3.3.2	Fitting model	46
3.3.3	Effect of extraction on BG solids extraction yield%	49
3.3.4	Total phenolic content (TPC) in BGEs	51
3.3.5	Total flavonoids (TFC) in BGEs	53
3.3.6	Ferric reducing antioxidant power (FRAP) in BGEs	55
3.3.7	Scavenging power of BGEs	57
3.3.8	Optimization of UAE process	59
3.4	Conclusion	61

CHAPTER 4 - CHARACTERIZATION AND OPTIMIZATION OF PRESSURIZED LIQUID EXTRACTION OF ANTIOXIDATIVE POLYPHENOLIC COMPOUNDS OBTAINED FROM MOMORDICA CHARANTIA

4.1	Introduction	62
4.2	Materials and methods	62
4.2.1	Chemicals, reagents and sample preparation	62
4.2.2	Conventional extraction method	63
4.2.3	Pressurized liquid extraction	63
4.2.4	Total Yield	64

4.2.5	Total Phenolic Content.....	65
4.2.6	Total Flavonoid Content	66
4.2.7	Ferric Reducing/antioxidant Power (FRAP) Assay	66
4.2.8	Free Radical Scavenging Activity.....	67
4.2.9	Experimental Design and Statistical Analysis	68
4.3	Results and discussion.....	70
4.3.1	Fitting the Models	70
4.3.2	Effects of extraction parameters on total yield	72
4.3.3	Effects of extraction parameters on total phenolic content.....	74
4.3.4	Effects of extraction parameters on total flavonoid content	77
4.3.5	Effects of extraction parameters on Ferric Reducing/antioxidant Power.....	80
4.3.6	Effects of extraction parameters on Radical Scavenging Activity.....	82
4.3.7	Optimization of extraction process	84
4.4	Conclusion.....	87

CHAPTER 5 - NANO ENCAPSULATION OF OBTAINED EXTRACT USING ELECTROSPRAYING METHOD

5.1	Introduction	88
5.2	Materials and Methods	88
5.2.1	Chemicals and reagents.....	88

5.2.2	Choice of crude extract for encapsulation purpose	89
5.2.3	Electrospraying system setup	89
5.2.4	Production of nanoparticles via electrospraying technique	90
5.2.5	Scanning electron microscopic (SEM) analysis.....	91
5.2.6	Transmission electron microscopic (TEM) analysis	91
5.2.7	Encapsulation efficiency determination	92
5.2.8	Atomic force microscopic (AFM) analysis	92
5.2.9	Attenuated total reflectance Fourier transform infrared spectroscopic analysis	93
5.2.10	Thermogravimetric Analysis	93
5.2.11	Differential scanning calorimetry (DSC)	93
5.2.12	Functional/Shelf Stability of Encapsulated Shell-Core Structure.....	94
5.2.13	Statistical design.....	94
5.3	Results and discussion	95
5.3.1	Surface morphology and particle size analysis of beads	95
5.3.2	Transmission Electron microscopy	98
5.3.3	Atomic Force Microscopy	99
5.3.4	Encapsulation Efficiency	100
5.3.5	ATR-FTIR spectra.....	101
5.3.6	Thermogravimetric analysis	104

5.3.7	Differential scanning calorimetry	106
5.3.8	Functional Stability of encapsulated extracts.....	108
5.4.	Conclusion.....	109

CHAPTER 6 - NANO ENCAPSULATION OF OBTAINED EXTRACT USING ELECTROSPINNING METHOD

6.1	Introduction	110
6.2	Materials and Methods	110
6.2.1	Chemicals and Reagents	110
6.2.2	Pure and Coaxial Fiber Production	111
6.2.3	Analytical and characterization.....	111
6.3	Results and Discussion.....	112
6.3.1	Surface morphology and particle size analysis of beads.....	112
6.3.2	Transmission electron microscopy.....	116
6.3.3	Atomic Force Microscopy.....	117
6.3.4	Encapsulation Efficiency	118
6.3.5	ATR-FTIR spectra	119
6.3.6	Thermogravimetric analysis.....	121
6.3.7	Differential scanning calorimetry analysis.....	122
6.3.8	Functional Stability of Encapsulated Shell-Core Structure	124
6.4	Conclusion.....	126

CHAPTER 7 - CONCLUSION AND RECOMMENDATIONS

7.1 Conclusion..... 127

7.2 Further Recommendations 128

REFERENCES 129

APPENDICES

LIST OF PUBLICATIONS

LIST OF TABLES

	Page
Table 2.1 List of major phytochemicals extracted from BG and their therapeutic effects.	6
Table 2.2 Ultrasound wave in acoustic span	11
Table 3.1 Experimental domain of Box-Behnken design.	35
Table 3.2 Box–Behnken design matrix and responses obtained at different experimental conditions	47
Table 3.3 Estimated coefficients of the fitted second order polynomial models for yield%, TPC, TFC, FRAP and IC50	49
Table 3.4 Estimated predicted and observed values within their intervals	60
Table 4.1 Experimental domain of central composite design (CCD)	64
Table 4.2 Central composite design (CCD) of the observed responses under different experimental conditions	70
Table 4.3 Estimated coefficients of the fitted second order polynomial models for Yield, TPC, TFC, FRAP and RSA%	72
Table 4.4 Estimated predicted and observed values within their intervals	86
Table 5.1 List of different variable used to obtain optimal hollow particles	90
Table 5.2 Antioxidative properties of PLE obtained Bitter gourd extract (BGE) before and after encapsulation process	101
Table 6.1 Antioxidative properties of PLE obtained Bitter gourd extract (BGE) before and after coaxial encapsulation process	119

LIST OF FIGURES

	Page
Figure 2.1 (a) BG flower, (b) Unripe White BG fruit (c) Unripe green BG fruit and (d) ripened BG fruit	5
Figure 2.2 (a) Cavitation caused by ultrasound (b) Microstreaming	12
Figure 2.3 Schematic diagram of liquid driven ultrasonic system (Sonochemistry Centre 2007)	14
Figure 2.4 Schematic diagram of magnetostrictive ultrasonic system (Morko America 2010)	15
Figure 2.5 Schematic diagram of electrostrictive system (Cleaning technologies group, 2012)	16
Figure 2.6 An schematic view of UAE effects in plant tissue matrix	18
Figure 2.7 Schematic diagram of static pressurized liquid extraction system setup (Mustafa and Turner 2011)	21
Figure 2.8 A schematic view of (a) electrospinning setup and associated components and (b) forces involved during electrospinning process (Khalf and Madihally 2017)	26
Figure 3.1 Single factor effect of solvent to solid ratio on (a) Yield%, (b) TPC, (c) TFC, (d) FRAP and (e) IC ₅₀	42
Figure 3.2 Single factor effect of processing temperature on (a) Yield%, (b) TPC, (c) TFC, (d) FRAP and (e) IC ₅₀	43
Figure 3.3 Single factor effect of calorimetric power on (a) Yield%, (b) TPC, (c) TFC, (d) FRAP and (e) IC ₅₀	45

Figure 3.4	Single factor effect of processing time on (a) Yield%, (b) TPC, (c) TFC, (d) FRAP and (e) IC ₅₀	46
Figure 3.5	Response surface plots illustrating the interactive effects of different extraction parameters on extraction yield%.	51
Figure 3.6	Response surface plots illustrating the interactive effects of different extraction parameters on TPC.	53
Figure 3.7	Response surface plots illustrating the interactive effects of different extraction parameters on TFC.	55
Figure 3.8	Response surface plots illustrating the interactive effects of different extraction parameters on FRAP.	57
Figure 3.9	Response surface plots illustrating the interactive effects of different extraction parameters on IC ₅₀ .	59
Figure 4.1	Response surface plots illustrating the interactive effects of different extraction parameters on extraction yield	74
Figure 4.2	Response surface plots illustrating the interactive effects of different extraction parameters on total phenolic content	77
Figure 4.3	Response surface plots illustrating the interactive effects of different extraction parameters on total flavonoid content	79
Figure 4.4	Response surface plots illustrating the interactive effects of different extraction parameters on ferric reducing/antioxidant power.	81
Figure 4.5	Response surface plots illustrating the interactive effects of different extraction parameters on radical scavenging activity%	84

Figure 5.1	Schematic view of the electrospinning system setup	89
Figure 5.2	SEM micrographs of empty gelatin beads at concentrations of (a) 5%, (b) 8%, (c) 10% and (d) 15%	96
Figure 5.3	SEM micrographs of gelatin beads (a) without encapsulation, (b) 5% encapsulation, (c) 10% encapsulation and (d) 15% encapsulation	97
Figure 5.4	Particle size distribution of (a) pure gelatin bead vs encapsulated beads with 5% extract core loading, (b) encapsulated beads with 5% extract core loading vs encapsulated beads with 10% extract core loading and (c) encapsulated beads with 10% extract core loading vs encapsulated beads with 15% extract core loading	98
Figure 5.5	TEM micrographs of gelatin beads (a) without encapsulation, (b) with 5% core loading, (c) with 10% core loading and (d) with 15% core loading	99
Figure 5.6	Topographical micro images of gelatin bead (a) without encapsulation, (b) with 5% core loading, (c) with 10% core loading and (d) with 15% core loading	100
Figure 5.7	FTIR spectra of (a) Bitter gourd extract, (b) Empty gelatin bead, (c) Gelatin beads encapsulated with 5% extract (d) Gelatin beads encapsulated with 10% extract and (e) Gelatin beads encapsulated with 15% extract	103
Figure 5.8	DTG (a) and TGA (b) thermographs of bitter gourd extract	106

	(BGE), gelatin powder (GP), empty gelatin bead (EGB), bead with 5% BGE (GBG5%), bead with 10% BGE (GBG10%) and bead with 15% BGE (GBG15%),	
Figure 5.9	DSC heating curve of gelatin powder (GP), empty gelatin bead (EGB), bead with 5% BGE (GBG5%), bead with 10% BGE (GBG10%) and bead with 15% BGE (GBG15%).	107
Figure 6.1	SEM micrographs of pure gelatin fibers at concentrations of (a) 30%, (b) 35%, (c) 40% and (d) 45%	113
Figure 6.2	SEM micrographs of (a) empty coaxial fibers,(b) coaxial fibers with 5% encapsulate loading (c) coaxial fibers with 10% encapsulate loading and (d) coaxial fibers with 15% encapsulate loading	115
Figure 6.3	Fiber size distribution of (a) empty coaxial vs 5% BGE encapsulated coaxial fiber (b) 5% BGE encapsulated coaxial fiber vs 10% BGE encapsulated coaxial fiber (c) 10% BGE encapsulated coaxial fiber vs 15% BGE encapsulated coaxial fiber and (d) empty coaxial vs 15% BGE encapsulated coaxial fiber	116
Figure 6.4	TEM micrographs of coaxial gelatin/ zein fibers encapsulated with (a) 5% crude extract (COE5%), (b) 10% crude extract (COE10%) and (c) 15% crude extract (COE15%)	117
Figure 6.5	Topographical micro images of core-shell zein/ gelatin fibers (a) without encapsulation (b) with 5% BGE encapsulate (c) with	118

	10% BGE encapsulate and (d) with 15% BGE encapsulate	
Figure 6.6	FTIR spectra of (a) Empty gelatin fiber (b) Empty zein fiber, (c) Empty coaxial fiber (d) Coaxial fiber with 5% extract loading (e) Coaxial fiber with 10% extract loading and (f) Coaxial fiber with 15% extract loading	120
Figure 6.7	DTG (a) and TGA (b) thermographs empty coaxial fibers (ECOF), coaxial fiber with 5% BGE (COE5%), coaxial fiber with 10% BGE (COE10%) and coaxial fiber with 15% BGE (COE15%)	122
Figure 6.8	First heating (a) and second heating (b) scans of empty coaxial fibers (ECOF), coaxial fiber with 5% BGE (COE5%), coaxial fiber with 10% BGE (COE10%) and coaxial fiber with 15% BGE (COE15%)	123

LIST OF ABBREVIATIONS

A	Absorbance
ADP	Average Diameter of Particle
AFD	Average Fiber Diameter
AFM	Atomic Force Microscopy
ANOVA	Analysis of Variance
AO	Antioxidant
AP	Adequate Precision
ASE	Accelerated Solvent Extractor
ATP	Adenosine Triphosphate
ATR-FTIR	Attenuated Total Reflection Fourier Transmission Infrared Spectroscopy
BBD	Box–Behnken design
BG	Bitter Gourd
BGE	Bitter Gourd Extract
CAE	Chlorogenic Acid Equivalent
CAT	Catalase
CCD	Central Composite Design
CHEST	Centre for Herbal Standardization
COE	Coaxial Encapsulated Fiber
C.V.%	Correlation Variation %
DPLE	Dynamic mode Pressurized Liquid Extraction
DPPH	2,2-Diphenyl-1-Picrylhydrazyl

DSC	Differential Scanning Calorimetry
ECOF	Empty Gelatin/ Zein Fibers
EE%	Extraction Efficiency
EEF	Encapsulation Efficiency
EGB	Empty Gelatin Bead
ETD	Everhart-Thornley Detector
FE-SEM	Field Emission Scanning Electron Microscopy
FR	Fermi Resonance Doublet
FRAP	Ferric Reducing Antioxidant Potency of Plasma
GAE	Gallic Acid Equivalent
GBG	Gelatin Encapsulated Bitter Gourd
GF	Gelatin Fiber
GP	Gelatin Powder
GPx	Glutathione Peroxidase
GRx	Glutathione Reductase
H ₂ O ₂	Hydrogen peroxide
HBA	Hydroxybenzoic
HCA	Hydroxycinnamic
HIU	High Intensity Ultrasound
IC ₅₀	Half inhibitory Concentration
LIU	Low Intensity Ultrasound

NADPH	Nicotinamide Adenine Dinucleotide Phosphate
O_2^-	Superoxide Anion Radical
OAQ	Oxidized Antioxidant
OPT	Optimum
PA	Phenolic Acids
PI	Prediction Interval
PLE	Pressurized Liquid Extraction
PZT	Lead Zirconate Titanate
QE	Quercetin Equivalent
RNS	Reactive Nitrogen Species
ROS	Reactive Oxygen Species
RSA	Radical Scavenging Activity
RSM	Response Surface Methodology
SFA	Single Factor Analysis
SLV/SOL	Solvent to Solid Ratio
SOD	Superoxide Dismutase
SWE	Subcritical Water Extraction
T_c	Crystallization Temperature
T_g	Glass Transition Temperature
T_m	Melting Temperature
T_{max}	Maximum Degradation Temperature
TE	Trolox Equivalent
TEM	Transmission Electron Microscopy

TFC	Total Flavonoid Content
TGA	Thermogravimetric Analysis
TPC	Total Phenolic Content
TPTZ	2,4,6-Tris(2-pyridyl)-s-Triazine
UAE	Ultrasound Assisted Extraction
US	Ultrasound

**KESAN PENGEKSTRAKAN BERTEKANAN DAN KAEDAH ENKAPSULASI
ELEKTROHIDRODINAMIK PADA SIFAT PENGOKSIDAAN BAGI
EKSTRAK BUAH *Momordica charantia* L.**

ABSTRAK

Objektif utama kajian ini adalah untuk menghasilkan model pengekstrakan dibantu tekanan bagi antioksidan polifenolik daripada peria katak sebagai model sayur-sayuran seperti buah-buahan dan seterusnya untuk mencirikan kaedah enkapsulasi nano elektrohidrodinamik dalam matriks polimer semula jadi. Metodologi permukaan tindak balas telah digunakan untuk mengkaji dan mengoptimumkan kesan masa pengekstrakan, suhu dan daya kuasa terhadap kalorimetrik ke atas jumlah kandungan fenolik, jumlah kandungan flavonoid, cerakin penurunan ferik/cerakin kuasa antioksidan dan aktiviti pembasmian radikal bagi ekstrak bantuan ultrasonik peria. Kondisi pengekstrakan optimum dicapai pada kuasa induksi 52.00 W, masa pengekstrakan 20 min dan suhu 60 °C. Tambahan pula, analisis statistik mendedahkan bahawa sifat-sifat antioksidan ekstrak adalah berhubung kait dengan kesan kuasa input dan suhu berbanding masa pemprosesan. Pengekstrakan cecair bertekanan bagi sebatian antioksidan dari buah peria dalam pelarut etanol akueus diselidik menggunakan metodologi permukaan tindak pada skala makmal. Kecekapan pengekstrakan dioptimumkan dengan mengukur jumlah kandungan fenolik, jumlah kandungan flavonoid, cerakin penurunan ferik cerakin kuasa antioksidan dan aktiviti pembasmian radikal. Kondisi pengekstrakan optimum dicapai pada kepekatan etanol 80%, masa pengekstrakan 10 min dan pada suhu 160 °C. Analisis statistik menunjukkan bahawa sifat antioksidan bagi ekstrak peria sangat berhubung kait dengan

suhu pengekstrakan dan kepekatan etanol yang positif berbanding masa pemprosesan. Kajian ini menggambarkan bahawa kedua-dua pengekstrakan bantuan ultrasonik dan pengekstrakan cecair bertekanan mempunyai potensi untuk mengekstrak sebatian antioksidan daripada sayuran buah-buahan tropika dengan cara yang dipercepat. Walau bagaimanapun, pengekstrakan cecair bertekanan menunjukkan keberkesanan yang lebih tinggi dari segi kuantiti hasil dan masa pemprosesan yang diperlukan. Proses semburan elektro dilakukan pada 20 kV, 0.5 mL/h dan 10 cm masing-masing bagi voltan, kadar aliran dan jarak pemancar/ pengumpul dan telah di enkapsulasi dengan ekstrak peria pada kadar 5 hingga 15% (w/w%). Analisis morfologi menunjukkan kejayaan penghasilan dan enkapsulasi nanosfera. Analisis spektroskopi menunjukkan tiada interaksi kimia di antara bahan teras dan dinding. Kestabilan termal dan kekristalan partikel yang dienkapsulasi meningkat. Kandungan fenolik dan aktiviti antioksida ekstrak yang dienkapsulasi menunjukkan kestabilan yang lebih tinggi semasa tempoh penyimpanan berbanding dengan BGE yang tidak dienkapsulasi. Struktur fiber nano koaksial zein / gelatin dihasilkan pada 20 kV, 0.5 mL/h dan 10 cm, masing-masing bagi voltan, kadar aliran dan jarak pemancar/pengumpul. Fiber gelatin telah dienkapsulasi dengan ekstrak peria pada kadar pemuatan 5% hingga 15%. Analisis morfologi mengesahkan fabrikasi struktur dwilapisan dan enkapsulasi ekstrak. Analisis termal mengesahkan bahawa proses enkapsulasi dalam fiber telah berlaku menyebabkan sedikit peningkatan bagi kestabilan haba. Tambahan lagi, enkapsulasi telah meningkatkan kestabilan antioksida ekstrak semasa penyimpanan.

**IMPACT OF PRESSURIZED EXTRACTION AND
ELECTROHYDRODYNAMIC ENCAPSULATION METHODS ON
ANTIOXIDATIVE PROPERTIES OF *Momordica charantia* L. FRUIT
EXTRACT**

ABSTRACT

The objectives of this study were first to model pressure assisted extraction of polyphenolic antioxidants from bitter gourd (BG) as a model fruit-like vegetable and secondly to characterize electrohydrodynamic nanoencapsulation methods within natural polymeric matrices. Response surface methodology (RSM) was used to investigate and optimize the impact of extraction time, temperature and induced calorimetric power on total phenolic content (TPC), total flavonoid content (TFC), Ferric reducing/antioxidant power assay (FRAP) and Radical scavenging activity (RSA) of BG ultrasonic assisted extract (UAE). The optimal extraction condition was reached at 52.00 W of induced power, extraction time of 20 min and temperature of 60 °C. Furthermore, statistical analysis revealed that antioxidative attributes of extracts were correlated with the effect of power input and temperature rather than processing time. Pressurized liquid extraction (PLE) of antioxidant compounds from BG fruits in the aqueous ethanolic solvent was investigated using RSM at a laboratory scale. Extraction efficiency was optimized by measuring the TPC, TFC, FRAP and RSA. The optimal extraction conditions were reached at 80% ethanol concentration, 10 min extraction time and at 160 °C of temperature. Statistical analysis revealed that antioxidative attributes of bitter gourd extract were strongly ($P < 0.05$) correlated with positive extraction temperature and

ethanol concentration effect rather than processing time. These studies illustrated that UAE and PLE both have potential to extract antioxidant compounds from tropical fruit vegetables in an accelerated manner. However, PLE demonstrated higher efficacy in terms of yield and required processing time. Electrospraying process was conducted at 20 kV, 0.5 mL/ h and 10 cm of voltage, flow rate and emitter/collector distance, respectively and were encapsulated with bitter gourd extract (BGE) at 5 to 15% (w/w%) rate. Morphological analysis demonstrated successful production and encapsulation of spheres. Spectroscopic analysis indicated no chemical interactions between core and wall materials. The thermal stability and crystallinity of encapsulated particles increased. Phenolic content and antioxidative activity of the encapsulated extract showed higher stability during the storage period in comparison to non-encapsulated BGE. Coaxial shell core zein/ gelatin nano fiber structure was produced at 20 kV, 0.5 mL/ h and 10 cm of voltage, flow rate and emitter/collector distance, respectively. The gelatin fiber was encapsulated with BGE at 5% to 15% loading rate. The morphological analysis confirmed fabrication of the bilayer structure and extract encapsulation. The thermal analysis confirmed that encapsulation process within the fibers had occurred; resulting in a slight thermal stability increase. Furthermore, encapsulation had increased antioxidative stability of extracts during storage.

CHAPTER 1

INTRODUCTION

1.1 Background

Bitter gourd (*Momordica charantia* L.) has been prominently used as a popular folk remedy across the south/south-east Asia region (Horax *et al.*, 2010). Many studies have shown that antioxidative properties of BG fruit are mostly due to the relatively high content of polyphenolic compounds present in them (Kubola and Siriamornpun 2008, Kenny *et al.*, 2013, Wu and Ng 2008). Therefore, many researchers have dealt with understanding the effects of various extraction methods on bioactive compounds obtained from BG fruit and their antioxidant attributes. The extraction processes were conventionally conducted through heating, boiling and refluxing methods (Li *et al.*, 2005, Wang *et al.*, 2008a, Bimakr *et al.*, 2011). These techniques are time-consuming, require high volumes of solvents and polyphenolic compounds could be lost due to hydrolysis, ionization and oxidation (Ignat *et al.*, 2011, Shan *et al.*, 2012, Huie 2002). Furthermore, the effects of processing parameters on the extracts obtained were merely studied on single factor basis without considering their interactional effects and the effects of multiple variables on extractability. These issues resulted in the search for a simple, accelerated and eco-friendly extraction method, which could be easily upscaled for industrial purposes. UAE and PLE are suitable pressure assisted extraction methods which could increase extraction rate and efficiency and be used as part of a continuous extraction platform. However, the effect of processing parameters on antioxidant compounds from a

fruit like vegetable such bitter gourd plant has not yet been investigated or modeled in a multilateral manner.

Furthermore, antioxidative properties of obtained compounds within extracts could not be fully harnessed, due to their sensitivity to light and oxygen, unless encapsulated within a biopolymer matrix. Conventional encapsulation methods used currently in food and nutraceutical sectors are spray drying, freeze drying, emulsification and coacervation (Ezhilarasi *et al.*, 2013). Despite their benefits, each of these technologies possesses a number of drawbacks limiting their application as an antioxidative compound encapsulation method. For instance, spray drying is not suitable for encapsulating heat sensitive material and is limited to certain wall material (Desai and Jin Park 2005). Meanwhile, coacervation is time consuming, costly, requires cross-linking of proteins and the stability of encapsulates must be retained in a very narrow pH range (Kralovec *et al.*, 2012). Freeze drying is rather the most time consuming and costly method of all encapsulation methods; exceeding other techniques by 30 to 50 times in investment and cost of opportunity expenses (Desobry *et al.*, 1997, Durance and Yaghmaee 2011). Therefore, a cost-effective encapsulation method which could be used at industrial scale and retain functional properties of the extract is required. Electrohydrodynamic methods could serve as suitable nonthermal alternative nano encapsulation method where a variety of polymeric geometries could be produced. However, very few studies have dealt with electrohydrodynamic encapsulation of antioxidative compounds especially crude extracts making it an emerging nonthermal technology.

1.2 Objectives

The objectives of the present study were to:

- 1) Characterize, model and optimize ultrasonic assisted extraction of bitter gourd fruit antioxidant compounds using response surface methodology
- 2) Characterize, model and optimize pressurized liquid extraction of bitter gourd fruit antioxidant compounds using response surface methodology
- 3) Compare the extraction efficiency of ultrasonic assisted extraction and pressurized liquid extraction methods
- 4) Produce, encapsulate and characterize gelatin nano spheres
- 5) Produce, encapsulate and characterize coaxial shell core (zein/gelatin) nano fibers
- 6) Study the antioxidative stability of the encapsulated nanostructures during storage

CHAPTER 2

LITERATURE REVIEW

2.1 Bitter Gourd

2.1.1 Etymology and morphology

Bitter gourd (*Momordica charantia* L.) (BG) is a monoecious, flowering, tendril-bearing vine belonging to Cucurbitaceae family (Joseph and Jini 2013, Beloin *et al.*, 2005). BG is indigenous to India, however, it could be found in tropical/sub-tropical regions of Malaysia, China, Africa, South America, Thailand as well as Caribbean (Grover and Yadav 2004). BG may be referred as bitter melon, balsam pear, karela, kugua, peria or pare depending on the region they are cultivated (Gupta *et al.*, 2010). The scientific name "*Momordica*" meaning "to bite" is depicted from the jagged-edged leaves which consist of three to seven deeply separated lobes (Grover and Yadav 2004).

BG fruit is commonly used as an ingredient for culinary and medicinal purposes in the Oriental Asia and West Africa. They have a distinctive oblong shape which resembles a cucumber (9 to 60 cm in length) with the warty surface (Lucas *et al.*, 2010). Depending on the variety, the unripe fruit is emerald green or white in color which will become orange-yellow once they ripen (Grover and Yadav 2004) (Figures 2.1 a-d). BG fruits have a distinguished bitter taste which becomes more prominent as they ripen (Grover and Yadav 2004).



Figure 2.1 (a) BG flower, (b) Unripe White BG fruit (c) Unripe green BG fruit and (d) ripened BG fruit

2.1.2 Medicinal applications of BG

BG is valued and used as a popular folk remedy wherever it is grown or cultivated (Horax *et al.*, 2010, Beloin *et al.*, 2005). In China, the seed and fruit are used for antiviral/immune-potentiating purposes as well as prevention and treatment of fever, polydipsia, diarrhea, colic, infections and diabetes (Grover and Yadav 2004, Fang *et al.*, 2012). In Indian traditional medicine, BG has been used to treat diabetics, dysmenorrhea, eczema, gout, jaundice, leucorrhoea, hemorrhoid, pneumonia, psoriasis and scabies (Basch *et al.*, 2003). In Turkish indigenous medicine, the ripe fruits are used topically for healing wounds and treating peptic ulcers and tumors (Alam *et al.*, 2009). Some studies have reported antifertility, abortifacient and birth controlling properties of BG leaf and fruit in females and sperm lowering effect on males (Tse *et al.*, 1999, Mossa 1985, Grover

and Yadav 2004). Furthermore, in some other cultures, they are used for relieving painful menstruation and facilitating childbirth (Beloin *et al.*, 2005).

Recent studies have shown that BGE contains several nutrients and bioactive compounds such as essential amino acids, carotenoids, folic acid, electrolytes, minerals and vitamins C and A which are considered beneficial to health (Habicht *et al.*, 2011, Hsu *et al.*, 2013). Phytochemicals isolated from the pulp, seeds, leaves and vines exhibit therapeutic effects such as antidiabetic, anticancer, antiviral, anti-inflammatory and hypolipidemic functionalities (Nerurkar *et al.*, 2008, Solinas *et al.*, 2010, Ono *et al.*, 2009) (Table 2.1).

Table 2.1 List of major phytochemicals extracted from BG and their therapeutic effects.

Therapeutic effect	Compound	Plant tissue Source
Anti-diabetic	Momordicoside (types Q, R, S,T), Poly peptide-P, karaviloside XI, Momordin (type I,II), alkaloids (vicine), and triterpenoids (Charantin), Saponin	Fruit, Leaf and seed
Antiviral	MAP30, α -momorcharin, β -momorcharin, γ -momorcharin, napinlike RIP, kuguacin 12 and 14, lectin, RNase-MCL	Fruit, Leaf and seed
Antimicrobial	MAP30, momordicine (Types I and II), chitinase	Fruit, Leaf and seed
Anti-tumour	Triterpene (types 1 and 2), Momordin I, cylglucosylsterols, lectin α -momorcharin, β -momorcharin, γ -momorcharin, napinlike RIP, RNase-MCL	Fruit, Leaf and seed
Hypoglycemic	Poly peptide-P, momordicosides (S, T), alkaloids, and triterpenoids	Fruit, Leaf and seed

2.2 BG antioxidant profile and potency

Few studies have dealt with profiling antioxidants and characterizing their properties in the extracts obtained from BG plant seeds, leaves and flesh (Wu and Ng 2008, Kubola and Siriamornpun 2008). These studies have reported potent antioxidative and radical scavenging activities of BGEs; making them potentially valuable functional and nutraceutical ingredients (Kubola and Siriamornpun 2008). The compounds responsible for mentioned properties mainly belong to flavonoids, polyphenols, polysaccharides and triterpenoids groups (Haque *et al.*, 2011, Panda *et al.*, 2015, Liu *et al.*, 2014). In this context, polyphenolic compounds namely gallic acid, caffeic acid, catechin, gentisic acid, chlorogenic acid and epicatechin are found most abundantly in BG plant tissue. Horax *et al.* (2005) reported that the total polyphenol compound concentrations in the seed, fruit inner tissue and flesh ranged from 470-800, 450-890 and 640-890 mg chlorogenic acid equivalent (CAE)/ 100 gr of dried extract respectively depending on their varieties. These results coincided with Kenny *et al.* (2013) results where polyphenolic compounds were reported to be the main antioxidative compound. Therefore, the antioxidative capacity of BGEs is defined and correlated with the phenolic content and reactivity (Kubola and Siriamornpun 2008, Othman *et al.*, 2007). Tan *et al.* (2014) reported that aqueous extract of BG fruit at its optimized conditions had a TPC, DPPH and FRAP content of 10.6 ± 0.2 mg GAE /g, 58.6 ± 1.0 μ mol TE/ g and 91.9 ± 1.8 μ mol TE/ g, respectively. The obtained values were either equal or higher than other organic solvents (acetone, n-butanol, 80% ethanol, methanol) used as a benchmark control. Wu and Ng (2008) extracted Taiwanese BG fruits by macerating the dried fruit powder in water (100 °C, 1hr) and ethanol (ambient conditions, 6 days). The TPC content of the aqueous extract was reported 5.1 g GAE/100

g while ethanolic extracts were slightly higher (6.2 g GAE/100 g) respectively. However, maximal TFC of 6.20 g QE/100g and half maximum inhibitory content (IC₅₀) of 0.157 mg/mL was achieved through the aqueous extraction process. Shan et al. (2012) optimized extraction parameters during ethanol modified supercritical carbon dioxide method (SC-CO₂) of BG fruits and achieved a TFC 15.47 mg/mL and radical scavenging activity% (RSA%) of $96.14 \pm 1.02\%$ at 1.2 mg/mL of extract concentration.

The antioxidative potency of extracts originated from different parts of BG varies based on the assay used. However, studies have mostly reported that leaves and fruits have the highest antioxidative and radical scavenging capacity. Kubola et al. (2008) reported that the leaves extract had the highest antioxidative activity based on the 1,1-Diphenyl-2-picrylhydrazyl (DPPH) radical scavenging and ferric reducing power methods. However, in the same study green bitter melon fruits extract expressed greater antioxidative activity based on β -carotene-linoleate bleaching assay.

2.6 Downstream processes of bioactive compounds

2.3.1 BG bioactive compound extraction methods

Natural polyphenolic bioactive compounds including BG are conventionally extracted from plant tissues through heating, boiling and refluxing methods (Li *et al.*, 2005, Wang *et al.*, 2008a, Bimakr *et al.*, 2011). However, these techniques are time-consuming, require high volumes of solvents and polyphenolic compounds are lost during the process due to hydrolysis, ionization and oxidation (Ignat *et al.*, 2011, Shan *et al.*, 2012, Huie 2002). Furthermore, nonpolar organic solvents such as chloroform and dichloromethane used through conventional method are highly toxic and prolonged exposure to them could result

in the lung, liver and pancreas cancer (Pitipanapong *et al.*, 2007). These issues have resulted in seeking greener methods involving simultaneous use of accelerated extraction methods and less hazardous solvents (e.g. water, ethanol and methanol). Among the vast number of emerging extraction methods, ultrasound-assisted extraction (UAE) and pressurized liquid extraction (PLE) have gained attention (Wang and Weller 2006). UAE has the potential to facilitate extraction process from plant tissues such as BG fruit. Mass transfer across cell membranes is enhanced due to vigorous liquid circulation, disruption of cell walls and reduction in particle size (Rathod and Rathod 2014). UAE efficiency is correlated with ultrasound (US) intensity, treatment time/ temperature, type of solvent used and its ratio to solid matter (Ramić *et al.*, 2015). PLE has become an attractive alternative extraction method to obtain plant bioactive extracts in comparison with conventional near ambient temperature and atmospheric pressure methods (Santos *et al.*, 2012, Tierney *et al.*, 2013). This is mainly due to the use of highly pressurized solvents maintained in a liquid state at temperatures above their atmospheric boiling point, resulting in facilitated extraction of phytochemicals without risking their chemical integrity (Mustafa and Turner 2011, Heffernan *et al.*, 2014).

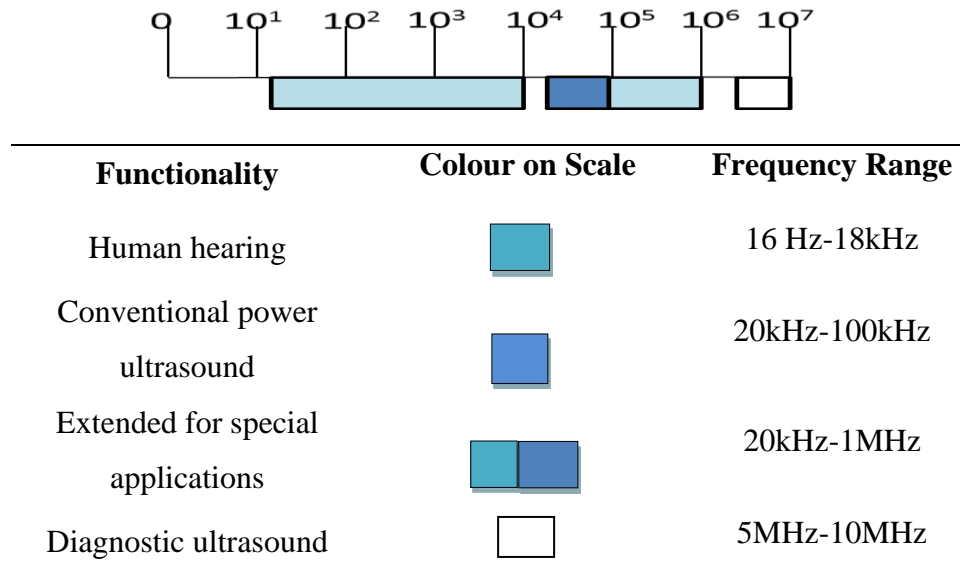
2.3.2 Ultrasound Assisted Extraction

2.3.2.1 Ultrasonic waves

Ultrasonic waves are circular, elastic waves with frequencies greater than 18 kHz (Table 2.2) (Mulet *et al.*, 1999). The vibrations produced by US propulsion could not be heard by humans since the frequencies are well above the normal hearing range (0.20-20 kHz) (Halliday *et al.*, 1996). Kocis and Figura (1996) categorized US waves into two types based on their frequency, velocity, and amplitude:

- 1) Low-intensity ultrasound waves (LIU) with frequencies higher than 100 kHz and intensities lower than 1 W/cm^2 . Such waves are mostly used for quality assurance tests and non-destructive analysis methods to evaluate factors such as composition, structure and the flow rate of foods (Povey and McClements, 1988). It has been reported that this range may be used as a processing aid besides diagnostic applications (Juliano *et al.*, 2011).
- 2) High-intensity ultrasound waves (HIU) with frequencies in the range of 20-100 kHz and intensities higher than 1 W/cm^2 ($10\text{--}1000\text{ W/cm}^2$) which are usually used as a source of energy. They can break down intermolecular bonds. In the food sector (dairy and meat), HIU is used for lowering microbial load and enzyme inactivation (Floros and Liang, 1994; Lopez *et al.*, 1994; Gallego, 1998). Cavitation phenomena are expected when induced power within the liquid media is higher than 10 W/cm^2 having the potential to alter the physical and chemical properties of the substances (Roberts and Wiltshire, 1990; McClements, 1995; Mason *et al.*, 1998).

Table 2.2 Ultrasound wave in acoustic span



2.3.2.2 Principles

Ultrasound waves are propagated by a series of compression and rarefaction cycles with a sinusoidal trend. As shown in Figure 2.2 acoustic streaming or micro streaming occurs at low intensities as the wave shears inside the liquid (Tho *et al.*, 2007). By increasing the amplitude, the rarefaction cycle overcomes the attractive forces between molecules. Consequently, the local pressure over the expansion phase decreases to amounts lesser than the vapor pressure of the liquid phase, resulting in cavitation bubbles. Transient or stable cavities are generated when acoustic energy overcomes the cavitation threshold (Ashokkumar and Grieser 2007). During the expansion phase vapor enters the bubbles from the medium which would lead to bubble rise. The vapor is not completely exhausted from bubbles during the consecutive compressions, which is due to the increase of the surface area. This rise can be the result of rectified diffusion and/or bubble coalescence pathways (Ashokkumar and Grieser 2007). As the transient bubble rises, it reaches a specific size (resonance size) throughout the compression/rarefaction cycle. In

this phase the oscillation of the bubble wall matches the sound frequency applied, thus the structure collapses during single compression (Moholkar *et al.*, 2000). Each collapsed cavitation bubble turns into a hotspot which generates heat and the shear is forced up to 2000-5000 K and 2000 atm, respectively (Figure 2.2a). The collapse occurs in a short period of time ($1\mu\text{s}$) in a near-adiabatic heating circumstance resulting in high local temperature (Ashokkumar and Grieser 2007). The generated energy induces chemical and mechanical alterations as well as an electrical field at the interface during bubble collapse (Patist and Bates 2008, Margulis and Margulis 2004). At lower intensities ($1\text{-}3\text{ W/cm}^2$) bubbles oscillate in a nonlinear trend around their stable size for many compression/rarefaction cycles without imploding leading to microstreaming (Ashokkumar and Grieser 2007) (Figure 2.2 b). The stable growth and shrinkage of micro streamers cause increments in temperature and pressure, which can influence the chemical reactions. Furthermore, stable cavitation is witnessed when applied frequency is higher than 200 kHz. When the bubble reaches the resonance size range it collapses but not as violently as transient bubbles do (Yasui 2002).

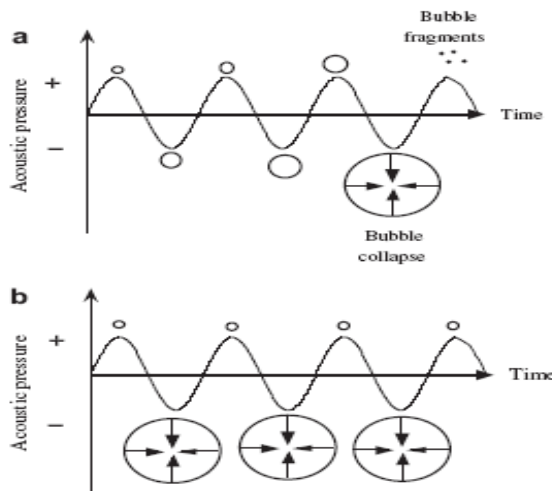


Figure 2.2 (a) Cavitation caused by ultrasound (b) Microstreaming

2.3.2.3 Ultrasound device setup

Different device setups are being used for transmitting ultrasonic sound waves in the liquid medium. Despite having differences in their design, ultrasound generating systems consist of three main parts: generator, transducer and coupler (Frame, 1994).

The generator should be a reliable source of energy, generating electrical or mechanical signals throughout the process. These pulses are sent to the transducer where are converted to sound energy in the ultrasonic frequency range. Acoustic, circular waves are transmitted by the coupler through the surrounding media. The transducers are classified into three main groups of (a) liquid driven, (b) magnetostrictive and (c) electrostrictive (piezoelectric) based on the technologies applied.(Leadeley and Williams 2006).

a. Liquid driven

In this system, the fluid is pushed through an orifice, against a metallic blade resulting into its propulsion at ultrasonic frequencies (Figure 2.3). The liquid driven system resembling a whistle is very robust and can work for consecutive hours. However, pumping is required which makes it suitable for processes such as homogenization which involves mixing (Leadeley and Williams 2006).

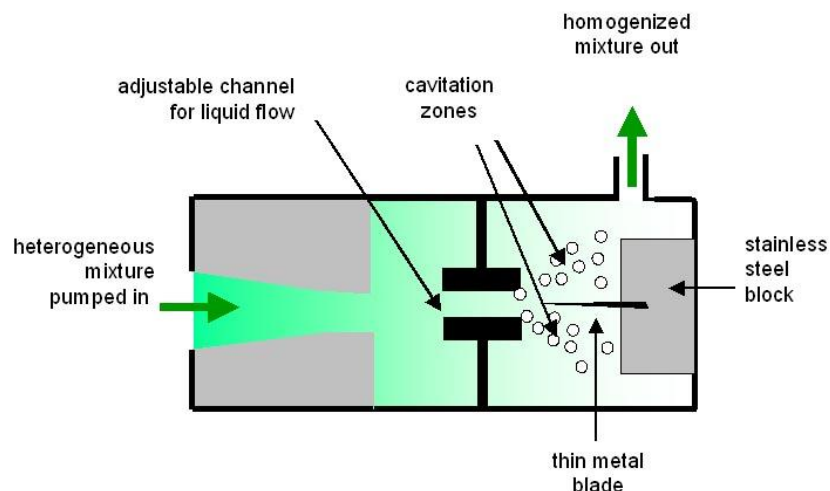


Figure 2.3 Schematic diagram of liquid driven ultrasonic system (Sonochemistry Centre 2007)

b. Magnetostrictive

This system is based on the magnetostrictive transformer principle where the magnetic field is applied to a coil surrounding the ferromagnetic material. The electrical current is passed through the wires generating a magnetic field inducing structural deformation and alteration in the ferromagnetic material (Figure 2.4) (Frame 1994). Magnetostrictive systems are rigged systems which can work for long periods. However, the system operating frequency and energy efficiency is limited and does not exceed more than 100 kHz and 60%, respectively. Furthermore, heat build-up is widely witnessed in these types of transducers (Povey and McClements 1988).

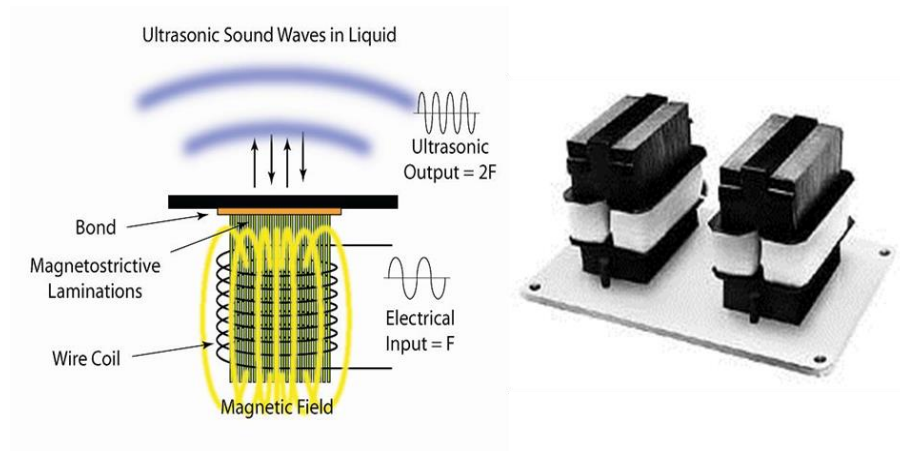


Figure 2.4 Schematic diagram of magnetostrictive ultrasonic system (Morko America 2010)

c. Electrostrictive (Piezoelectric)

This system is designed based on the electrostrictive transformer principle and is constructed of a single or double layer piezoelectric plate material, surrounded by electrodes (Leadeley and Williams 2006). The electrostrictive materials are normally made of ceramic compounds such as lead metaniobate, lead zirconate titanate (PZT) or barium titanate entrapped between aluminum and steel blocks. High-frequency current is sent through electrodes (Figure 2.5) resulting in electrical field generation. This generated electrical field induces mutual attraction forces between polarized molecules forcing the ferroelectric material to resonate. Electrostrictive transducers are the most widely used system setups due to higher energy efficiency (85-90%) and frequencies (up to 150 MHz). However, these systems are not as robust as the previously discussed systems and cannot withstand temperatures above 85 °C.

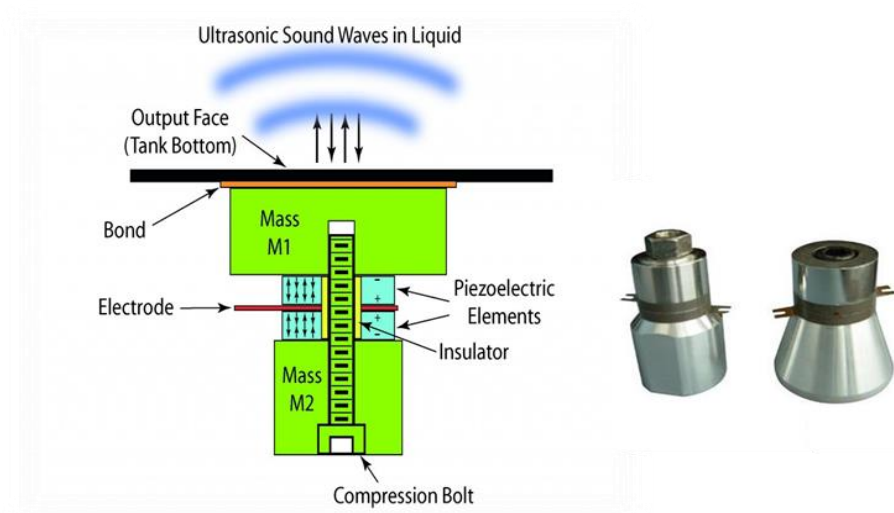


Figure 2.5 Schematic diagram of electrostrictive system (Cleaning technologies group, 2012)

2.3.2.4 UAE of bioactive compounds

UAE has gained much attention among many other emerging technologies for replacing conventional bioactive extraction methods (Wong Paz *et al.*, 2015). This issue is mainly due to improved extraction yield at relatively short time, higher selectivity, low solvent consumption and high quality extracts obtained using ultrasound technology (Chen *et al.*, 2007, Chemat *et al.*, 2011, Zhao and Baik 2012, Chavan and Singhal 2013, Ramić *et al.*, 2015). Furthermore, simple and low-cost installation and operation procedure of ultrasound facilities have made them an attractive substitutive technology (Bimakr *et al.*, 2012, Wang and Weller 2006).

Enhanced extraction of bioactive compounds from plant materials by ultrasound is mainly attributed to the propagation of pressure waves within the solvent and consequent occurrence of cavitation phenomena. These mechanical effects result in vigorous shear forces within the active site facilitating solvent penetration within the sample matrix and

increasing mass transfer of extractable materials (Li *et al.*, 2012). Furthermore, the localized pressure generated by the violent collapse of cavitation bubbles at or in close vicinity to the surface of the plant tissue can result in cell wall rupture increasing the mass transfer rate (Briones-Labarca *et al.*, 2015). As indicated by Vilku *et al.* (2008) and Goula (2013) the implosion of cavitation bubbles generates macro-turbulence, high-velocity inter-particle collisions, and perturbation in microporous particles of the biomass, which accelerates the eddy diffusion and internal diffusion. Moreover, cavitation near the solvent-matrix interface results in passage of fast-moving currents of solvent within the cavities located at the surface. On the other hand, cavitation occurrence on the plant tissue surface results in impingement of microjets resulting in surface peeling, erosion, and particle breakdown. This process provides exposure to new surfaces and consequent increase in mass transfer rate. Apart from this, ultrasound waves facilitate swelling and hydration processes, essential for extraction of plant substrates, by enlargement of cell wall pores and reducing cell size (Goula 2013). In this sense, disruption of cellular structure, diffusion across plant cell walls and washing out of the contents occur more readily when compared with conventional methods. The mentioned mechanisms enhancing extraction of plant materials within the solvent during UAE has been summarized in Figure 2.6.

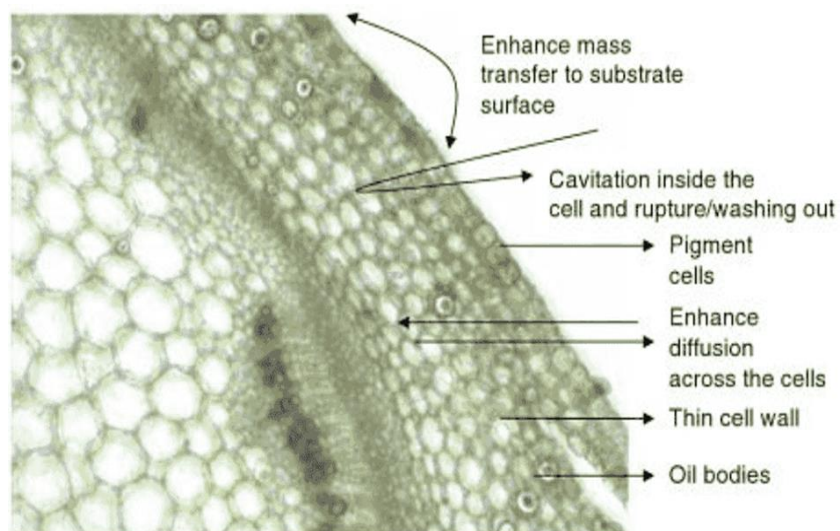


Figure 2.6 An schematic view of UAE effects in plant tissue matrix

Wong Paz et al. (2015) studied the impact of UAE (e.g. solid ratio, solvent concentration and extraction time) parameters on polyphenolic extraction process from a variety of desert plants indigenous to Mexico. They indicated that the main factor affecting extraction efficiency namely solvent ratio, treatment time and solid to solvent ratio varies from one plant to another. However, they reported that 40 minutes of UAE with 35% aqueous ethanol and 8 to 12 mL/g solvent to solid ratio was the most favorable phenolic compounds extraction condition. Samaram et al. (2015) reported that the yield and antioxidative capacity of extracted papaya seed oil were strongly correlated with extraction time and temperature. Fang et al. (2014) also reported that bioactive compound extraction yield and activity from false daisy plant were correlated with processing conditions.

2.3.3 Pressurized Liquid Extraction (PLE)

PLE is relatively a new concept in food technology where extraction occurs at high pressures and temperatures reaching near supercritical conditions (Mustafa and Turner 2011). PLE was originally developed for efficient extraction of environmental pollutants found in soil matrix, sewage sludge, sediments and fly ash. Furthermore, PLE has the potential to substitute conventional extraction techniques used in food, pharmaceutical and agriculture sectors. (Benthin *et al.*, 1999, Nemoto and Lehotay 1998). This is mainly due to the distinct nature of PLE; conducted based on static extraction principles at high pressure and superheated conditions (Wijngaard *et al.*, 2012, Mendiola *et al.*, 2007). Reduced extraction time, low solvent volume requirement and selectivity in separating a specific class of compound is due to the mentioned dual effect.

The key factors governing the extraction process often used for optimization purposes are the processing temperature, pressure, time and choice of solvent. However, it is worthy to mention that temperature and pressure of the choice dictate other processing variables during the extraction process. The use of solvents at temperatures above their atmospheric boiling point enhances the efficiency and selectivity of PLE. This issue is mainly due to the higher solubility, diffusivity and mass transfer of solute within the superheated solvent. Thermal energy interrupts analyte-matrix interactions by breaking Vander Waals forces, hydrogen bonding and dipole intramolecular attractions (Ong *et al.*, 2000). Furthermore, the activation energy of desorption process between the solute and matrix is reduced due to heat-induced disruption of the cohesive and adhesive interactions. Moreover, the viscosity and surface tension of the solvent in relation to the solute and matrix is reduced resulting in better solvent wetting and penetration properties.

High-pressure levels applied during PLE has a crucial impact on improving analyte solubility and desorption kinetics from the sample matrix. Elevated pressure levels allow the solvent to reach temperatures beyond their boiling point without undergoing a phase change. Besides this, pressurized superheated solvents have relatively lower surface tension enhancing their penetration kinetics through the matrix particles. Furthermore, high-pressure levels facilitate solvent access to the solute through physical disruption of the matrix and disruption of air bubble formation within its structure (Mustafa and Turner 2011).

2.3.3.1 PLE Equipment

The instruments used for PLE processing are either operated in batch; using static PLE or continuous modes; through dynamic PLE apparatus. Static systems are most commonly used for commercial purposes while no dynamic system setup has yet been designed for industrial-scale take-up. However, it is worthy to mention that recently some PLE devices have been manufactured which are able to operate in a dual static-dynamic mode.

In static mode, the extraction process is undertaken through one or several cycles using fresh solvent for each cycle. Static systems consist of stainless steel or titanium extraction cells, the heating compartment (Oven or carousel), cooling system, static and relief valves and a pump to fill the cells (Figure 2.7).

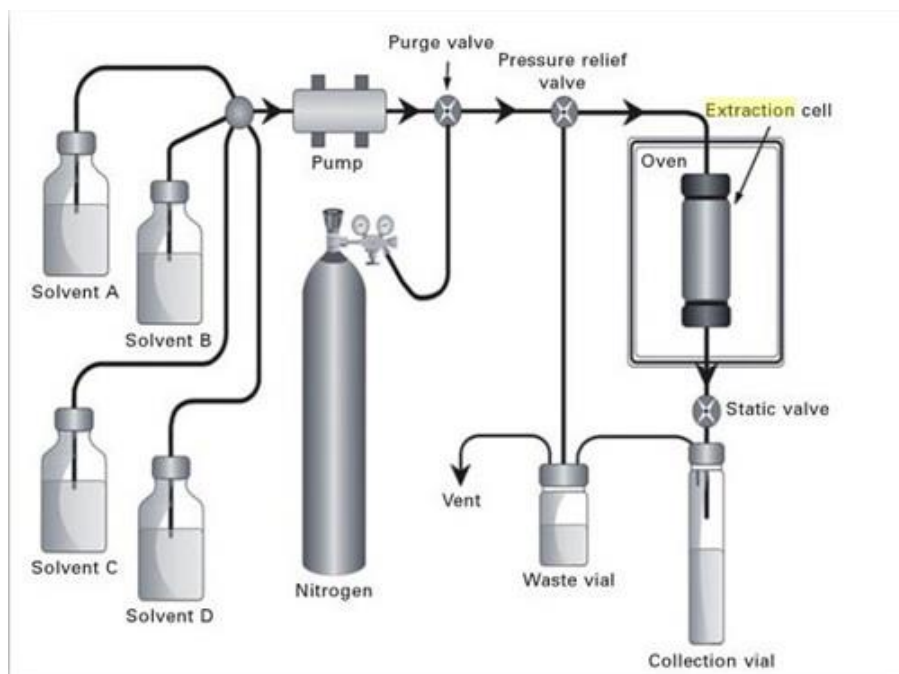


Figure 2.7 Schematic diagram of static pressurized liquid extraction system setup (Mustafa and Turner 2011)

Dynamic and static devices are quite similar in design, however dynamic setups consist of sophisticated high pressure or HPLC pumps as well as pressure restrictors. This is due to the different mode of action during dynamic PLE where the solvent is continuously pumped through the extraction vessels.

2.3.3.2 PLE of phytochemicals

Over the past few years, the interest in using PLE as a bioactive compounds extraction method has significantly increased. This is mainly due to the use of highly pressurized solvents maintained in a liquid state at temperatures above their atmospheric boiling point, resulting in facilitated extraction of phytochemicals without risking their chemical integrity (Mustafa and Turner 2011, Heffernan *et al.*, 2014). Furthermore, automated nature of PLE requires less treatment time and solvent volumes has made this technology

favorable. Apart from this, PLE of plant materials at temperatures above 100 °C results in extracts with high antioxidant activity. This could be due to the occurrence of various reactions generating antioxidant capable compounds (Ahmadian-Kouchaksaraie *et al.*, 2016, Hossain *et al.*, 2011). Besides this, minimal sample preparation requirements has made PLE suitable for extraction of oxygen and light-sensitive compounds

Recent studies have reported that various bioactive compounds such as polyphenols, carotenoids, essential oils and lipids were successfully extracted using PLE. The flexibility and selectivity offered by PLE are mainly due to its compatibility with numerous polar and nonpolar solvent systems (e.g. Ethanol, methanol, ethyl acetate acetone, petroleum ether, diethyl ether, tetrahydrofuran and hexane). Budrat and Shotipruk (2009) studied the effect of various parameters on PLE of phenolic compounds from BG fruit in comparison to conventional methods. However, the effect of extraction parameters on phenolic compounds of extracts was not mathematically optimized and the effect of other solvents at near critical conditions was left undiscussed. Benthin et al. (1999) compared PLE extraction of four medicinal herbs (*Hyperici herba*, *Hippocastani semen*, *Cardui mariae fructus* and *Curcumae rhizome*) with the conventional extraction method. They reported that PLE method was more superior in extracting bioactive chemicals (essential oils, polycyclic phenols, phenylpropane and flavonolignans) in terms of extraction rate, time and solvent consumption. Ong et al. (2000) studied the impact of temperature, the volume of solvent required and particle size on dynamic mode PLE (DPLE) of berberine and aristolochic acids (I & II) and optimized it accordingly. They reported that extraction efficacy was higher in comparison with UAE and conventional Soxhlet extraction methods. Machado et al. (2015) studied the impact of different solvents systems on PLE efficacy and antioxidative capacity of phenolic and monomeric

anthocyanin compounds from blackberries. The most optimal extraction condition was achieved through aqueous ethanol solvent at 100 °C resulting in total phenolic, monomeric anthocyanin, antioxidant activity and global yield of 7.36 mgGAE/g, 1.02 mg C3GE/g fresh residue, 76.03 μ mol TE/g and 6.33%, respectively. It is worthy to mention that the authors reported higher extraction efficiency at all PLE conditions in comparison to conventional extractions used as the benchmark process (Soxhlet and maceration).

2.4 Encapsulation processes

In the past few years, the need for developing micro/nano scale structures to protect plant-based bioactive components has gained much attention. Encapsulation techniques provide barriers between sensitive bioactive materials and the environment (de Vos *et al.*, 2010). This initiative improves the end product properties by masking unpleasant flavor/odor, improving the stability, enhancing core material bioavailability and targeted delivery (Champagne and Fustier 2007, Gouin 2004).

A range of different techniques are being used for micro and nanoencapsulation of food bioactive compounds including spray drying, spray chilling, freeze drying, emulsification, coacervation and nanoprecipitation (Ezhilarasi *et al.*, 2013). There are certain advantages and disadvantages in using each of these techniques. For instance, spray drying has the advantages of low operational cost, availability of the machinery, reliability in operation and ability to control the particle size of spray dried emulsion (Kaushik *et al.*, 2015). However, this method is not suitable for encapsulating heat sensitive material and is limited to certain wall material (Desai and Jin Park 2005). Furthermore, nanoencapsulation through spray drying requires modifications in the dryer

system setup (Anu Bhushani and Anandharamakrishnan 2014). The main advantages of coacervation techniques over spray drying are obtaining encapsulates with lower particle size, higher payload and prevention of core material migration through the shell. However, this method is time-consuming, costly, requires cross-linking of proteins and the coacervates retain their stability in a very narrow pH range (Kralovec *et al.*, 2012). Freeze drying provides a practical solution for preservation and encapsulation of thermolabile and expensive material within a coating material. However, the main drawbacks of this process are the rather high cost of operation (30 to 50 times of conventional spray drying process) and long drying cycle period ranging from 48 to 72 hours (Desobry *et al.*, 1997, Durance and Yaghmaee 2011). Furthermore, additional costs and difficulties associated with storage and transportation of the produced dehydrated material makes it less attractive for industrial uptake (Madene *et al.*, 2006). The issues described above results in a pursuit of an alternative method which is green, cost-effective and comparatively rapid.

2.4.1 Electrohydrodynamic Technologies

Electrohydrodynamic methods including electrospraying and electrospinning are simple, versatile and cost-effective methods for synthesizing ultrafine fibers, particles and capsules at micron, submicron and nanoscale (Pérez-Masiá *et al.*, 2015). The principle behind electrospraying and electrospinning process is virtually of the same essence (Anu Bhushani and Anandharamakrishnan 2014). Spun or sprayed material is formed as the result of high electric potential field induction between a polymer droplet and grounded collector interface (Li *et al.*, 2011). Electrospinning and electrospraying processes are